

NONCOHERENT SEQUENCE ESTIMATION: A COMPARISON

Robert Schober[†], Lutz H.-J. Lampe[†], and Gerald Enzner[‡]

[†] Laboratorium für Nachrichtentechnik, Universität Erlangen–Nürnberg

[‡] Institut für Nachrichtengeräte und Datenverarbeitung, RWTH Aachen

Abstract — In this paper, three previously proposed non-coherent sequence estimation (NSE) schemes are compared for two important applications: convolutionally coded MPSK transmission over the AWGN channel and differential MPSK transmission over intersymbol interference (ISI) channels. We show that the influence of the rectangular observation window employed by all considered NSE schemes can be described by the same nonrecursive amplitude and phase reference symbols. In order to increase the computational efficiency, we propose an infinite but exponentially decaying observation window. In this case, the reference symbols can be generated in a recursive way. We investigate how the performance of the considered NSE schemes is influenced by the type of observation window used, the observation window size, and reduced-state decoding.

1. Introduction

In this paper, noncoherent sequence estimation (NSE) for convolutionally coded M -ary phase-shift keying (MPSK) transmission over the additive white Gaussian noise (AWGN) channel and uncoded differential MPSK (MDPSK) transmission over intersymbol interference (ISI) channels is considered. For both applications NSE is a favorable choice if carrier synchronization is too complex or not feasible. The main advantage of NSE (and any noncoherent receiver) is that all problems associated with synchronization circuits such as acquisition, tracking, false lock detection, false lock prevention, etc., are circumvented [1].

In contrast to coherent MLSE, optimum NSE cannot be implemented using the Viterbi algorithm (VA) since a recursive metric calculation is not possible, i.e., a tree search is necessary and complexity increases exponentially with the number of transmitted symbols. Another problem is that for derivation of the optimum NSE metric the channel phase is assumed to be constant for the entire transmission. In practice, however, the channel phase is often slowly time-variant and optimum NSE suffers from severe performance degradations.

In the last decade a variety of suboptimum NSE schemes [2, 3, 4, 5, 6, 7, 8, 9, 10, 11, 12, 13, 14] have been proposed to overcome the aforementioned problems. These NSE schemes are derived from optimum NSE and most of them use an *observation window* of a finite size N , $N \geq 2$, whereas the schemes in [6] and [13] employ an infinite but exponentially decaying observation window with a forgetting factor α , $0 \leq \alpha < 1$. Both N and α enable a trade-off between power efficiency for constant phase and robustness against phase variations.

The above cited suboptimum NSE schemes may be divided into three classes. The schemes proposed in [3, 7] belong to the first class, where a limited tree search is used for decoding. Since, in general, it is more convenient to use a trellis for decoding, we do not consider this approach in the following. The NSE schemes of the second class [5, 9, 10] are motivated by multiple-symbol detection [15, 16], i.e., one branch in the decoding trellis

embraces several branches of the original code (ISI) trellis. Therefore, a decoding trellis with the same number of states as the original trellis results. However, the number of branches originating from each trellis state is higher than in the original trellis. E.g., in the ISI case the number of trellis branches per decoded symbol is $M^{N-2}/(N-1)$ times higher than in a corresponding coherent receiver [10]. Unfortunately, for these schemes complexity reduction is very difficult since a reduction of branches or states leads to a significant performance degradation. Thus, in practice, NSE schemes belonging to the second class can only be applied for small observation windows and will also not be regarded in the following. The NSE schemes of the third class [2, 4, 8, 11, 13, 14] use an augmented code (ISI) trellis to account for the influence of the received symbols contained in the observation window, i.e., the number of states is increased whereas the number of branches per state is the same as in the original trellis. In this case, complexity (number of states) can be controlled easily by *per-survivor processing* [17] (cf. [4, 8, 11, 12, 13, 14]). Therefore, these NSE schemes are well suited for implementation and will be compared in this paper.

Our contributions are as follows. First, we highlight the similarities and the differences of the NSE schemes proposed by Raphaeli et al. [8, 12] (referred to as R-NSE), Colavolpe and Raheli [11]¹ (CR-NSE), and Zhang et al. [14] (ZMLG-NSE). Second, we generalize the concept of the exponentially decaying observation window [6, 13], which conveniently enables the recursive calculation of the reference symbols, to all considered NSE schemes. Last, we investigate how a reduction of the observation window size or the number of states affects the performance of the considered NSE schemes.

2. Transmission Model

The considered discrete-time transmission model is depicted in Fig. 1. All signals are represented by their complex-baseband equivalents and T -spaced sampling is assumed. Thus, the received signal samples are given by

$$r[k] = e^{j\Theta} y[k] + n[k], \quad (1)$$

where k denotes the discrete-time channel symbol index. Θ and $n[k]$ are a constant uniformly distributed phase shift and white Gaussian noise, respectively. Due to an appropriate normalization $n[k]$ has variance $\sigma_n^2 = N_0/E_S$, where N_0 and E_S refer to the single-sided power spectral density of the underlying continuous-time passband noise process and the mean received energy per symbol, respectively. $y[k]$ is the received (noise-free) signal component which depends on the MPSK information symbols $a[i] \in \mathcal{A} = \{e^{j2\pi\nu/M} | \nu \in \{0, 1, \dots, M-1\}\}$ with discrete-time information symbol index i . The estimated information symbols $\hat{a}[\cdot]$ are delivered with a decision delay i_0 (cf. Fig. 1). In order to become more specific, in the following we distinguish two cases.

¹The schemes in [2] and [4] may be considered as special cases of the more general scheme of [11].

a) *Convolutionally coded MPSK transmission*: In this case, the code symbols $b[k]$ are generated by an M -ary *noncoherently non-catastrophic* convolutional encoder (CC) [8] from the information symbols $a[i]$. Here, a non-dispersive channel is presumed, i.e., $y[k] = b[k]$ is valid. For simplicity, we restrict ourselves to code rates $R_c = 1/\eta$, $\eta \in \{2, 3, \dots\}$. The constraint length of the code is denoted by L .

b) *MDPSK transmission over ISI channels*: For MDPSK transmission over ISI channels, a differential encoder (DE) is employed, i.e., $k = i$ holds and the MDPSK symbols are obtained from $b[k] = a[k] \cdot b[k-1]$. The noise-free symbols $y[k]$ are given by

$$y[k] = \sum_{l=0}^{L-1} h_l b[k-l], \quad (2)$$

where h_l , $0 \leq l \leq L-1$, denotes the coefficients of the discrete-time overall channel impulse response. Now, L refers to the length of the channel impulse response.

The CC and the combination of DE and discrete-time ISI channel can be modeled as a finite state machine, respectively, and thus, the same NSE techniques can be employed in both cases.

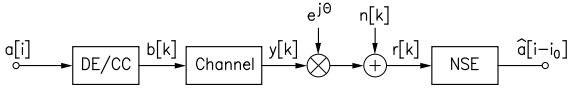


Figure 1: Block diagram of the transmission model.

3. Noncoherent Sequence Estimation

3.1. Optimum NSE

If we assume the transmission of a block of N_b information symbols which are collected in a vector \mathbf{a} , the block of estimated symbols $\hat{\mathbf{a}}$ can be obtained from the noncoherent maximum-likelihood decision rule [18, 10, 11]

$$\hat{\mathbf{a}} = \underset{\tilde{\mathbf{a}}}{\operatorname{argmin}} \{ \Lambda_{\text{ML}}[\eta(N_b + L - W)] \} \quad (3)$$

with the optimum metric

$$\Lambda_{\text{ML}}[\eta(N_b + L - W)] \triangleq \frac{1}{\sigma_n^2} \sum_{k=0}^{\eta(N_b+L-W)} |\tilde{y}[k]|^2 - \ln \left(\text{I}_0 \left(\frac{2}{\sigma_n^2} \left| \sum_{k=0}^{\eta(N_b+L-W)} r[k] \tilde{y}^*[k] \right| \right) \right) \quad (4)$$

where $\text{I}_0(\cdot)$ refers to the zeroth order modified Bessel function of the first kind and L denotes the constraint length of the code or the length of the ISI channel ($\eta = 1$ holds for the ISI case). For coded MPSK $W = 2$ is valid, whereas $W = 1$ is necessary for MDPSK since in the latter case the first transmitted symbol $b[0]$ is required as reference for the following symbols, i.e., $b[0]$ cannot be recovered at the receiver. The hypothetical noise-free symbols $\tilde{y}[k]$, $0 \leq k \leq \eta(N_b + L - W)$, are uniquely associated with a hypothetical information sequence $\tilde{\mathbf{a}}$ via convolutional encoding or via the DE and the channel impulse response. In practice, it is desirable to avoid the cumbersome modified Bessel function. For this purpose, two approximations are commonly used. Namely, $\ln(\text{I}_0(|x|))$ may be

approximated by $|x|^2$ or $|x|$ [8, 11]. The first approach only leads to acceptable results if the first sum in (4) is of no importance, i.e., if $|\tilde{y}[k]|$ is constant for all k and $\tilde{\mathbf{a}}$ (cf. [11, 12, 19]), which is e.g. true for ISI-free MPSK transmission. However, even if $|\tilde{y}[k]| = \text{const.}, \forall k$, holds, the second approximation is preferable since it leads to a better performance of the suboptimum NSE schemes derived from optimum NSE (cf. [11] for a comparison for CR-NSE). Therefore, in the following, $\ln(\text{I}_0(|x|)) \approx |x|$ is used exclusively and hence, the optimum metric may be replaced by the *quasi-optimum* metric

$$\Lambda'_{\text{ML}}[\eta(N_b + L - W)] = \sum_{k=0}^{\eta(N_b+L-W)} |\tilde{y}[k]|^2 - 2 \left| \sum_{k=0}^{\eta(N_b+L-W)} r[k] \tilde{y}^*[k] \right|. \quad (5)$$

Unfortunately, $\Lambda'_{\text{ML}}[\eta(N_b + L - W)]$ cannot be calculated recursively. Another problem is that performance degrades severely if the phase is not approximately constant over the entire block of transmitted symbols. In order to overcome these problems, three suboptimum NSE schemes are considered.

3.2. Suboptimum Schemes Using Nonrecursive Reference Symbols

In the following, three suboptimum schemes are discussed. These schemes are derived from optimum NSE but use a finite observation window of size N . We will show that in each case the influence of the $N-1$ previous signal samples received at times $k-N+1, k-N+2, \dots, k-1$ on the metric at time k can be subsumed in an amplitude and a phase reference symbol.

a) *ZMLG-NSE*: ZMLG-NSE has been recently proposed by Zhang et al. [14]. Here, the quasi-optimum metric is evaluated only for the N most recent observed signal samples $r[k-\nu]$, $0 \leq \nu \leq N-1$, i.e., the metric to be minimized is

$$\Lambda_{\text{ZMLG}}[k] \triangleq |\tilde{y}[k]|^2 + \tilde{y}_{\text{ref}}^2[k-1] - 2|r[k] \tilde{y}^*[k] + \tilde{q}_{\text{ref}}[k-1]|, \quad (6)$$

where the nonrecursive amplitude and phase reference symbols are given by

$$\tilde{y}_{\text{ref}}^2[k-1] \triangleq \sum_{\nu=1}^{N-1} |\tilde{y}[k-\nu]|^2 \quad (7)$$

and

$$\tilde{q}_{\text{ref}}[k-1] \triangleq \sum_{\nu=1}^{N-1} r[k-\nu] \tilde{y}^*[k-\nu], \quad (8)$$

respectively.

b) *R-NSE*: For R-NSE, which has been introduced by Raphaeli et al. [8, 12], the quasi-optimum metric for N observed signal samples is used as *incremental* metric

$$\lambda_{\text{R}}[k] \triangleq |\tilde{y}[k]|^2 + \tilde{y}_{\text{ref}}^2[k-1] - 2|r[k] \tilde{y}^*[k] + \tilde{q}_{\text{ref}}[k-1]| \quad (9)$$

and the *accumulated* metric to be minimized is calculated recursively from

$$\Lambda_{\text{R}}[k+1] = \Lambda_{\text{R}}[k] + \lambda_{\text{R}}[k], \quad (10)$$

i.e., *maximally overlapped observations* [8] are used.

c) *CR-NSE*: Colavolpe and Raheli defined the branch metric $\lambda'_{\text{CR}}[k] \triangleq \Lambda'_{\text{ML}}[k+1] - \Lambda'_{\text{ML}}[k]$ which is the difference

of two quasi-optimum metrics. If the *phase memory* [11] is limited to $N - 1$ symbols, the resulting branch metric $\lambda_{\text{CR}}[k]$ can be written as

$$\lambda_{\text{CR}}[k] = |\tilde{y}[k]|^2 - 2|r[k]\tilde{y}^*[k] + \tilde{q}_{\text{ref}}[k-1]| + 2|\tilde{q}_{\text{ref}}[k-1]|. \quad (11)$$

The accumulated metric is given by

$$\Lambda_{\text{CR}}[k+1] = \Lambda_{\text{CR}}[k] + \lambda_{\text{CR}}[k]. \quad (12)$$

From the above considerations it is obvious that the considered suboptimum NSE schemes are closely related. All schemes employ a nonrecursively generated phase reference symbol $\tilde{q}_{\text{ref}}[k-1]$. If the hypothetical symbols necessary for generation of $\tilde{y}[k-\nu]$, $1 \leq \nu \leq N-1$, coincide with the actually transmitted information symbols and the channel noise is neglected, $r[k-\nu] = e^{j\Theta}\tilde{y}[k-\nu]$, $1 \leq \nu \leq N-1$, is obtained. In this case, $\tilde{q}_{\text{ref}}[k-1] = e^{j\Theta} \cdot x$, $x \in \mathbb{R}^+$, results, i.e., $\tilde{q}_{\text{ref}}[k-1]$ provides an estimate for the phase difference between $r[\cdot]$ and $\tilde{y}[\cdot]$. ZMLG-NSE and R-NSE also require an amplitude reference symbol $\tilde{y}_{\text{ref}}^2[k-1]$, which allows a similar interpretation. Note that for ISI-free transmission both $|\tilde{y}[k]|^2$ and $\tilde{y}_{\text{ref}}^2[k-1]$ may be omitted in the above metrics (cf. (6), (9), (11)). For all considered suboptimum NSE schemes a trellis may be used for decoding. In order to limit the complexity, per-survivor processing [17] can be adopted, i.e., the hypothetical symbols $\tilde{a}[i-\nu]$, $0 \leq \nu \leq K$, are defined by the transition

$$\tilde{t}[i] \triangleq [\tilde{a}[i] \tilde{a}[i-1] \dots \tilde{a}[i-K]] \quad (13)$$

from state

$$\tilde{S}[i] \triangleq [\tilde{a}[i-1] \tilde{a}[i-2] \dots \tilde{a}[i-K]] \quad (14)$$

to state $\tilde{S}[i+1]$ in the underlying trellis diagram. The number of states is $Z = M^K$. For $\nu > K$ the hypothetical symbols $\tilde{a}[i-\nu]$ are replaced by estimated symbols $\hat{a}[i-\nu]$ taken from the surviving path terminating in $\tilde{S}[i]$.

3.3. Suboptimum Schemes Using Recursive Reference Symbols

Simulations show that for a constant channel phase all suboptimum NSE schemes discussed in Section 3.2 become more power efficient if the observation window size N is increased. However, at the same time the number of terms to be added for calculation of the amplitude and phase reference symbols also increases (cf. (7), (8)). To overcome this problem, for CR-NSE and MDPSK transmission over ISI channels an exponentially decaying infinite observation window has been proposed in [13] since for this type of window the reference symbols can be calculated recursively in a very efficient way. Here, we extend this concept to coded MPSK transmission and to ZMLG-NSE and R-NSE.

The reference symbols in (7), (8), can be obtained from the optimum reference symbols $\tilde{y}_{\text{ref}}^2[k-1] = \sum_{\nu=1}^{\infty} |\tilde{y}[k-\nu]|^2$ and $\tilde{q}_{\text{ref}}[k-1] = \sum_{\nu=1}^{\infty} r[k-\nu]\tilde{y}^*[k-\nu]$ by application of a rectangular window of length $N-1$. This measure limits the memory and thus, slow phase variations can be tolerated. However, from a practical point of view an exponentially decaying window is better suited. This leads to the modified reference symbols

$$\tilde{y}_{\text{ref}}^2[k-1] \triangleq \sum_{\nu=1}^{\infty} \alpha^{\nu-1} |\tilde{y}[k-\nu]|^2, \quad (15)$$

$$\tilde{q}_{\text{ref}}[k-1] \triangleq \sum_{\nu=1}^{\infty} \alpha^{\nu-1} r[k-\nu]\tilde{y}^*[k-\nu], \quad (16)$$

where α , $0 \leq \alpha < 1$, denotes a *forgetting factor* which also limits the memory.

From (15) and (16) we obtain the recursive relations

$$\begin{aligned} \tilde{y}_{\text{ref}}^2[k-1] &= \alpha \cdot \tilde{y}_{\text{ref}}^2[k-2] + |\tilde{y}[k-1]|^2, \\ \tilde{q}_{\text{ref}}[k-1] &= \alpha \cdot \tilde{q}_{\text{ref}}[k-2] + r[k-1]\tilde{y}^*[k-1] \end{aligned} \quad (17)$$

These recursive reference symbols are employed for ZMLG-NSE, R-NSE, and CR-NSE in the metrics given by (6), (9), and (11), respectively. The transitions and states can be defined as in the nonrecursive case (cf. (13), (14)). Each path in the trellis has its private reference symbols $\tilde{y}_{\text{ref}}^2[k-1]$ and $\tilde{q}_{\text{ref}}[k-1]$, which are updated according to (17) and (18) using the previous reference symbols $\tilde{y}_{\text{ref}}^2[k-2]$ and $\tilde{q}_{\text{ref}}[k-2]$ of the same path.

The number of arithmetic operations is independent of forgetting factor α but grows with observation window size N for the nonrecursive reference symbols. Thus, the savings in computational complexity offered by the recursive reference symbols increase with increasing power efficiency. A comparison of the nonrecursive and the recursive reference symbols also shows that both are identical for the special cases $N=2$ ($N \rightarrow \infty$) and $\alpha=0$ ($\alpha \rightarrow 1$).

It should be mentioned that a recursive phase reference symbol was also used in [6]. This scheme could also be obtained using our approach if we started from CR-NSE and used the approximation $\ln(I_0(|x|)) \approx |x|^2$.

4. Comparison of Suboptimum NSE Schemes

4.1. Observation Window Size and Forgetting Factor

From (6), (9), and (11) it can be seen that ZMLG-NSE and R-NSE/CR-NSE are affected quite differently by the reference symbols and thus, by N and α . For large values of N and α (and a sufficiently large number of states), in principle, all schemes can approach coherent MLSE, however, for practically interesting cases ($N \leq 20$ and $\alpha \leq 0.9$) there are important differences.

a) ZMLG-NSE

In this case, $\tilde{y}_{\text{ref}}^2[k-1]$ and $\tilde{q}_{\text{ref}}[k-1]$ are directly employed for calculation of the *accumulated* metric $\Lambda_{\text{ZMLG}}[k]$ (cf. (6)). Therefore, a reduction of N (α) does not only decrease the phase memory but also the code (ISI) memory taken into account for NSE. This causes a large performance degradation for practical values of N (α).

b) R-NSE and CR-NSE

(9) and (11) show that for R-NSE and CR-NSE only the *branch* metrics are affected directly by $\tilde{y}_{\text{ref}}^2[k-1]$ and $\tilde{q}_{\text{ref}}[k-1]$, i.e., the accumulated metric is influenced in an indirect way. As a consequence, a reduction of N (α) does **not** influence the code (ISI) memory taken into account for NSE. For this reason an acceptable performance of these schemes can also be expected for small values of N (α).

From the above considerations and our simulation results in Section 5, we can conclude that ZMLG-NSE can only be applied if the channel phase is approximately constant over that number of symbol intervals for which all paths in the trellis have merged. Unfortunately, this rules out

most practical interesting applications of NSE². Thus, for the rest of this section, we concentrate on R–NSE and CR–NSE.

4.2. Nonrecursive vs. Recursive Reference Symbols

In general, it is very difficult to quantify the influence of N or α due to the nonlinear character of NSE. Analytical results may be found in [8] and [21] for R–NSE and CR–NSE with nonrecursive reference symbols, respectively. In both cases, coded MPSK transmission over the non–dispersive AWGN channel is regarded.

Here, we want to emphasize the differences and similarities of nonrecursive and recursive reference symbols. For this, it is convenient to consider transmission over pure AWGN channels and ISI corrupted channels separately.

a) *Coded MPSK over AWGN channel*: In this case, only the phase reference symbol is of importance since $|\tilde{y}[k]| = 1$, $\forall \tilde{\mathbf{a}}$, is valid. For a simple comparison, we may calculate the signal–to–noise ratio (SNR) of the nonrecursive and the recursive reference symbol which is defined as

$$\text{SNR}_q \triangleq \frac{|\mathcal{E}\{\tilde{q}_{\text{ref}}[k-1]\}|^2}{\mathcal{E}\{|\tilde{q}_{\text{ref}}[k-1] - \mathcal{E}\{\tilde{q}_{\text{ref}}[k-1]\}|^2\}} \quad (19)$$

($\mathcal{E}\{\cdot\}$ denotes expectation), where $\tilde{y}[k] = y[k]$, i.e., $\tilde{\mathbf{a}}[k] = \mathbf{a}[k]$, $\forall k$, is assumed. Despite the convolutional coding, in general, $\mathcal{E}\{b[k]b^*[l]\} = 0$, $k \neq l$, is fulfilled. Thus, from (8) and (16) we obtain

$$\text{SNR}_q = \frac{N-1}{\sigma_n^2} \quad (20)$$

and

$$\text{SNR}_q = \frac{1+\alpha}{\sigma_n^2(1-\alpha)} \quad (21)$$

for the nonrecursive and the recursive reference symbol, respectively. Using (20) and (21), it can be easily shown that both reference symbols have the same SNR for

$$\alpha = 1 - \frac{2}{N}. \quad (22)$$

Extensive simulations have shown [22] (cf. also Section 5) that the SNR of the reference symbol is a meaningful performance measure for CR–NSE, i.e., if N and α are chosen according to (22), the receivers with nonrecursive and recursive reference symbol achieve approximately the same BER. On the other hand, for R–NSE, in general, the receiver with recursive reference symbol has a better performance than that with nonrecursive reference symbol if the parameters are chosen according to (22).

b) *MDPSK over ISI channels*: Because of the non–constant magnitude of $\tilde{y}[k]$, the SNR of the reference symbol is not a meaningful parameter for the BER performance if the channel is corrupted by ISI. Here, other properties of the reference symbol may dominate the performance. In particular, there are channel impulse responses (e.g. $h_0 = h_1 = 1/\sqrt{2}$, $L = 2$) for which $y[k] = \sum_{l=0}^{L-1} h_l b[k-l] = 0$ results for certain combinations of transmitted MPSK symbols $b[k-l]$, $0 \leq l \leq L-1$. This means that there are certain combinations of symbols $b[k-1]$, $b[k-2]$, \dots , $b[k-$

²In [14] uncoded quadrature amplitude modulation (QAM) is considered where paths merge quickly and acceptable performance of ZMLG–NSE can also be achieved for relatively small values of N (α). However, in that special case, sequence estimation is not necessary at all (cf. e.g. [20]).

$L - N + 2$] for which the nonrecursive phase reference symbol ((8)) is zero. Hence, the phase reference is lost and the occurrence of an error event becomes very likely. Since this loss of phase reference is independent of the channel noise variance, it leads to an error floor which is approximately proportional to $1/M^{N-1}$. For the recursive reference symbol with $\alpha > 0$ these problems do not exist. (16) shows that here an infinite number of (weighted) symbols are added, i.e., the probability that all of them vanish is zero.

On the other hand, if $y[k] \neq 0$, $\forall b[\cdot]$, is valid or if $y[k] = 0$ is very unlikely, which is true e.g. for time–variant fading channels, the respective schemes with nonrecursive and recursive reference symbol show a similar performance if N and α are chosen accordingly [23].

4.3. Influence of State Reduction

It has been shown in [8] and [11, 21] for R–NSE and CR–NSE, respectively, that both schemes can approach the performance of coherent MLSE if a full–state Viterbi algorithm is used for decoding. Unfortunately, in general, full–state NSE requires a larger number of states than coherent full–state MLSE. Therefore, in practice, reduced–state decoding is more interesting. For ISI channels a full reduction to only one state is possible. In this case, for both R–NSE and CR–NSE the same noncoherent decision–feedback equalizer (NDFE) results [24, 19]. However, if more than one state is used for decoding both schemes are different. Here, for simplicity, we consider ISI–free transmission. Thus, for R–NSE the simplified incremental metric $\lambda'_R[k] = -|r[k]\tilde{y}^*[k] + \tilde{q}_{\text{ref}}[k-1]|$ might be used. If we assume $N \gg 1$ or $\alpha \rightarrow 1$, $|\tilde{q}_{\text{ref}}[k-1]| \gg |r[k]\tilde{y}^*[k]|$ is valid as long as the majority of hypothetical/estimated information symbols, which are defined by the state/surviving path and used for generation of $\tilde{q}_{\text{ref}}[k-1]$, coincides with the actually transmitted information symbols. Thus, if we use the relation $|1+z| \approx 1 + \Re\{z\}$ ($\Re\{\cdot\}$ denotes the real part of a complex number), $z \in \mathbb{C}$, which holds for $|z| \ll 1$, we obtain

$$\begin{aligned} \lambda'_R[k] &= -|\tilde{q}_{\text{ref}}[k-1]| \cdot \left| 1 + \frac{r[k]\tilde{y}^*[k]}{\tilde{q}_{\text{ref}}[k-1]} \right| \\ &\approx -|\tilde{q}_{\text{ref}}[k-1]| - \Re \left\{ r[k]\tilde{y}^*[k] \frac{\tilde{q}_{\text{ref}}^*[k-1]}{|\tilde{q}_{\text{ref}}[k-1]|} \right\} \end{aligned} \quad (23)$$

The second term in (23) can be interpreted as coherent MLSE metric with incorporated phase estimation since $\tilde{q}_{\text{ref}}^*[k-1]/|\tilde{q}_{\text{ref}}[k-1]| \approx e^{-j\hat{\theta}}$ holds for the correct path for a constant channel phase. However, the first term $|\tilde{q}_{\text{ref}}[k-1]|$ is not present in the coherent MLSE metric. Therefore, if we employ per–survivor processing, erroneous estimated symbols in the surviving path do not only affect the phase estimate incorporated in the R–NSE metric but do also influence $\lambda'_R[k]$ via $|\tilde{q}_{\text{ref}}[k-1]|$. Our simulations show that this has a negative effect on the performance of R–NSE, i.e., if the simple reduced–state decoding algorithm based on per–survivor processing and discussed in Sections 3.2, 3.3 is employed, in general, the performance of a coherent receiver cannot be approached. For R–NSE this simple algorithm is similar to the *basic decision feedback algorithm* (BDFA) proposed in [25]. In [25] also more sophisticated reduced–state techniques are presented to overcome the limitations imposed by the R–NSE metric. However, these algorithms are more complex and we will show that they are not necessary if CR–NSE is employed.

If we make the same assumptions as above also for CR–NSE and use the simplified metric $\lambda''_{\text{CR}}[k] = -|r[k]\tilde{y}^*[k] + \tilde{q}_{\text{ref}}[k-1]| + |\tilde{q}_{\text{ref}}[k-1]|$, we obtain

$$\lambda''_{\text{CR}}[k] \approx -\Re \left\{ r[k]\tilde{y}^*[k] \cdot \frac{\tilde{q}_{\text{ref}}^*[k-1]}{|\tilde{q}_{\text{ref}}[k-1]|} \right\}, \quad (24)$$

i.e., the CR–NSE metric is identical with the coherent MLSE metric with incorporated phase estimation. Our simulations show that, in this case, the performance of coherent MLSE can be approached if N or α are chosen sufficiently large.

5. Simulation Results

a) *Coded MPSK over AWGN channel*: For coded QPSK transmission over the AWGN channel we adopt a code with $Z_c = 16$ states and generator polynomials $\mathbf{g}_1 = (1, 3, 3)$ and $\mathbf{g}_2 = (2, 3, 1)$ (base–4 representation) proposed in [8] ($L = 3$, $R_c = 1/2$). Extensive simulations using various codes showed that for all investigated NSE schemes a favorable trade–off between complexity and performance can be achieved by using $Z = M \cdot Z_c$ states for decoding [22]. Thus, in the following, $Z = 64$ states are adopted for all considered NSE schemes, whereas for coherent MLSE $Z = Z_c = 16$ states are employed for decoding, of course.

Fig. 2 shows BER vs. $10 \log_{10}(E_b/N_0)$ (E_b is the received energy per information bit) for ZMLG–NSE, R–NSE, CR–NSE, and coherent MLSE. For Figs. 2a) and b) nonrecursive and recursive reference symbols are used, respectively. Apparently, ZMLG–NSE degrades severely for small values of N and α (cf. Section 4.1). Even for $\alpha = 0.9$ ZMLG–NSE performs worse than CR–NSE with $\alpha = 0.3$. On the other hand, CR–NSE always outperforms R–NSE if the same value of N (α) is used in both cases. For the nonrecursive reference symbol with $N = 5$ and $N = 7$ there is a gap of approximately 0.75 dB between R–NSE and CR–NSE. In the recursive case, this gap is smaller, however, for R–NSE with $\alpha = 0.9$ there remains still a gap of 0.7 dB to coherent MLSE, whereas this gap is only 0.2 dB for CR–NSE with $\alpha = 0.9$. This supports our results from Section 4.3, i.e., R–NSE with simple state reduction techniques cannot approach coherent MLSE. Note that for CR–NSE the curves for $N = 3$ ($N = 5$) and $\alpha = 0.3$ ($\alpha = 0.6$) are approximately identical, i.e., (22) turns out to be a good rule of thumb in this case. This has been also confirmed for other codes in [22].

In Fig. 3, the robustness of the considered suboptimum NSE schemes against phase jitter is assessed. The same code as above is used and $10 \log_{10}(E_b/N_0) = 4$ dB is valid. Here, the phase $\Theta[k]$ is modeled as Wiener process, i.e., the sequence of phase changes is a white Gaussian process with variance σ_{Δ}^2 over T . The robustness against phase jitter decreases with increasing N and α . Obviously, the schemes with nonrecursive and recursive reference symbol show a similar robustness.

In [6], it was observed that NSE with recursive reference symbol is as sensitive to phase variations as coherent MLSE with a phase–locked loop (PLLs). However, in [6] α was chosen close to 1 ($\alpha = 0.96$) which explains the sensitivity of the resulting NSE scheme to phase variations. Note that NSE with a corresponding nonrecursive reference symbol (i.e., $N = 50$) would show a similar behavior.

In [12], it was reported that CR–NSE is more sensitive to phase variations than R–NSE. However, these results cannot be confirmed here. Fig. 3 shows that CR–NSE and R–NSE have a similar robustness against phase variations.

From Figs. 2, and 3 we conjecture that ZMLG–NSE is not well suited for practical applications and therefore, will not be considered in the following.

b) *Uncoded MDPSK over ISI channels*: Figs. 4a) and b) show BER vs. $10 \log_{10}(E_b/N_0)$ for nonrecursive and recursive reference symbols, respectively, for a channel with impulse response $h_0 = h_1 = 1/\sqrt{2}$ ($L = 2$) and QDPSK modulation, i.e., $y[k] = 0$ is possible. For equalization of ISI channels, in general, NSE achieves high performance if the same number of states is used like for coherent full–state MLSE [19]. Hence, here $Z = 4$ is adopted for both NSE and coherent MLSE. As predicted in Section 4.2b), both CR–NSE and R–NSE suffer from an irreducible error floor, which is approximately proportional to $1/4^{N-1}$, if nonrecursive reference symbols are used. The error floor is avoided if a recursive reference symbol with $\alpha > 0$ is employed. For $N = 2$ and $\alpha = 0$ the nonrecursive and the recursive reference symbols are identical and CR–NSE and R–NSE have practically the same performance for these parameters. In general, however, again CR–NSE outperforms R–NSE. For R–NSE also for $N = 10$ and $\alpha = 0.9$ a considerable gap to coherent MLSE remains.

Another possible field of application for NSE is mobile communications [23]. Further simulations have shown that R–NSE and CR–NSE achieve a similar performance for typical mobile channels [19].

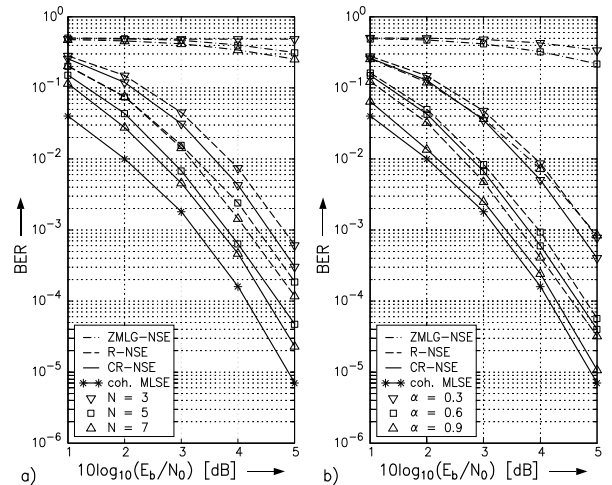


Figure 2: BER vs. $10 \log_{10}(E_b/N_0)$ for coded QPSK transmission with the considered NSE schemes ($Z = 64$) and coherent MLSE ($Z = 16$).

6. Conclusions

In this paper, ZMLG–NSE, R–NSE, and CR–NSE have been compared for coded MPSK transmission over the AWGN channel and uncoded MDPSK transmission over ISI channels. We have shown that all considered schemes employ nonrecursive amplitude and phase reference symbols but may be easily extended to incorporate recursive reference symbols which can be updated more efficiently. A detailed comparison has revealed that ZMLG–NSE is not well suited for most practical applications since it works only well as long as a relatively large observation window is used. However, this excludes channels with time–varying phase. R–NSE and CR–NSE are both well suited for application, however, if a simple reduced–state decod–

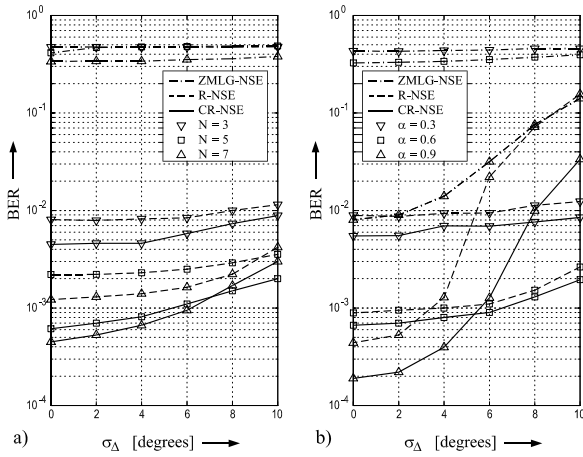


Figure 3: BER vs. jitter standard deviation σ_{Δ} per modulation interval T for coded QPSK transmission with the considered NSE schemes ($Z = 64$).

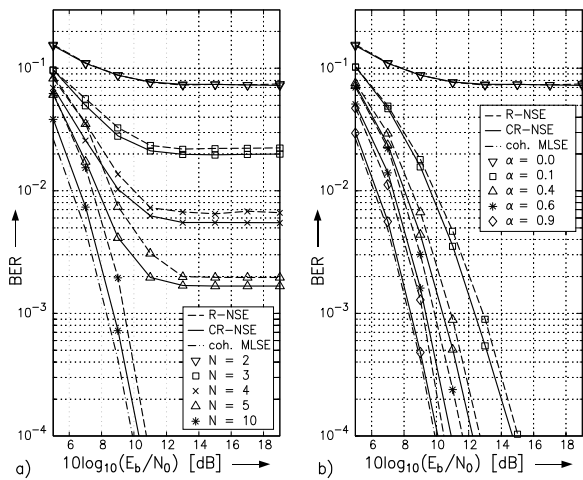


Figure 4: BER vs. $10 \log_{10}(E_b/N_0)$ for QDPSK transmission over an ISI channel with impulse response $h_0 = h_1 = 1/\sqrt{2}$ ($L = 2$).

ing algorithm based on per-survivor processing is applied, CR-NSE is preferable since it offers a better performance. It has also been shown that the recursive reference symbol compares favorably with the nonrecursive one and thus, can be recommended for all considered NSE schemes.

Acknowledgement

The authors would like to thank W. H. Gerstacker and J. B. Huber for many fruitful discussions throughout the development of this paper.

References

- [1] M. K. Simon, S. M. Hinedi, and W. C. Lindsey. *Digital Communication Techniques: Signal Design and Detection*. Prentice-Hall, Inc., Englewood Cliffs, New Jersey, 1994.
- [2] D. Makrakakis, A. Yongacoglu, and K. Feher. A Sequential Decoder for Differential Detection of Trellis Coded PSK Signals. In *Proceedings of the International Conference on Communications (ICC)*, pages 1433–1438, Philadelphia, June 1988.
- [3] S.T. Andersson and N.A.B. Svensson. Noncoherent Detection of Convolutionally Encoded Continuous Phase Modu-

- lation. *IEEE Journal on Selected Areas in Communications (JSAC)*, SAC-7:1402–1414, December 1989.
- [4] P.Y. Kam and H.C. Ho. Viterbi Detection with Simultaneous Suboptimal Maximum Likelihood Carrier Phase Estimation. *IEEE Transactions on Communications*, COM-36:1327–1330, December 1988.
- [5] D. Divsalar, M.K. Simon, and M. Shahshahani. The Performance of Trellis-Coded MDPSK with Multiple Symbol Detection. *IEEE Transactions on Communications*, COM-38:1391–1403, September 1990.
- [6] A. D'Andrea, U. Mengali, and G. Vitetta. Approximate ML Decoding of Coded PSK with No Explicit Carrier Phase Reference. *IEEE Transactions on Communications*, COM-42:1033–1039, February/March/April 1994.
- [7] T.R. Giallorenzi and S.G. Wilson. Noncoherent Demodulation Techniques for Trellis Coded M -DPSK Signals. *IEEE Transactions on Communications*, COM-43:2370–2380, August 1995.
- [8] D. Raphaeli. Noncoherent Coded Modulation. *IEEE Transactions on Communications*, COM-44:172–183, February 1996.
- [9] Y. Kofman, E. Zehavi, and S. Shamai (Shitz). nd -Convolutional Codes – Part I and II. *IEEE Transactions on Information Theory*, IT-43:558–589, March 1997.
- [10] W. Gerstacker, R. Schober, and J. Huber. Noncoherent Equalization Algorithms Based on Sequence Estimation. In *Proceedings of IEEE Global Telecommunications Conference (GLOBECOM)*, pages 3485–3490, Sydney, November 1998.
- [11] G. Colavolpe and R. Raheli. Noncoherent Sequence Detection. *IEEE Transactions on Communications*, COM-47:1376–1385, September 1999.
- [12] A. Ben-Zur and D. Raphaeli. Noncoherent Trellis Coded Amplitude-Phase Modulation. In *Proceedings of IEEE Global Telecommunications Conference (GLOBECOM)*, pages 2518–2522, Rio de Janeiro, December 1999.
- [13] R. Schober and W. H. Gerstacker. Metric for noncoherent sequence estimation. *IEE Electronics Letters*, 35(25):2178–2179, December 1999.
- [14] J. Zhang, S. Mei, J. Lu, and J. Gu. Burst demodulation of QAM with unknown carrier phase. *IEE Electronics Letters*, 35(24):2077–2079, November 1999.
- [15] S. G. Wilson, J. Freebersyter, and C. Marshall. Multi-Symbol Detection of M -DPSK. In *IEEE Global Telecommunications Conference (GLOBECOM)*, pages 47.3.1–47.3.6, Dallas, November 1989.
- [16] D. Divsalar and M. K. Simon. Multiple-Symbol Differential Detection of MPSK. *IEEE Transactions on Communications*, COM-38:300–308, March 1990.
- [17] R. Raheli, A. Polydoros, and C.-K. Tzou. Per-Survivor Processing: A General Approach to MLSE in Uncertain Environments. *IEEE Transactions on Communications*, COM-43:354–364, February/March/April 1995.
- [18] J.G. Proakis. *Digital Communications*. McGraw-Hill, New York, second edition, 1989.
- [19] R. Schober. *Noncoherent Detection and Equalization for MDPSK and MDAPSK Signals*. PhD Thesis, University Erlangen-Nürnberg, Shaker Verlag, July 2000.
- [20] R. Schober, W. H. Gerstacker, and J. B. Huber. Decision-feedback differential detection scheme for 16-DAPSK. *IEE Electronics Letters*, 34(19):1812–1813, September 1998.
- [21] G. Colavolpe and R. Raheli. Theoretical Analysis and Performance Limits of Noncoherent Sequence Detection of Coded PSK. *IEEE Transactions on Information Theory*, IT-46:1483–1494, July 2000.
- [22] G. Enzner. *Noncoherent Sequence Estimation for Coded $M(D)$ PSK and CPM Transmission*. Diplomarbeit (master project), Telecommunications Institute II, University Erlangen-Nürnberg, 2000.
- [23] R. Schober and W. H. Gerstacker. Noncoherent Adaptive Channel Identification Algorithms for Noncoherent Sequence Estimation. *IEEE Transactions on Communications*, 49, February 2001.
- [24] R. Schober and W. H. Gerstacker. Adaptive Noncoherent DFE for MDPSK Signals Transmitted Over ISI Channels. *IEEE Transactions on Communications*, COM-48:1128–1140, July 2000.
- [25] D. Raphaeli. Decoding Algorithms for Noncoherent Trellis-Coded Modulation. *IEEE Transactions on Communications*, COM-44:312–323, March 1996.